



Fracture Behavior of Carbon Nanotubes Containing Crack: Theoretical and Molecular Dynamics Analysis

Wu-Gui Jiang^{1,*}, Qiu-Wei Fu¹, Chuan Peng¹, Zheng Chang², and Hong-Ping Zhao^{2,*}

¹School of Aeronautical Manufacturing Engineering, Nanchang Hangkong University, Nanchang 330063, P. R. China

²Department of Engineering Mechanics, Tsinghua University, Beijing 100084, P. R. China

A theoretical model for predicting fracture behavior of carbon nanotubes (CNTs) with the effects of temperature and strain rate is presented based on kinetic analysis of fracture. The influences of assuming defects including a single crack, horizontal and vertical parallel double cracks in the CNTs are also discussed using quantized fracture mechanics (QFM) theory and molecular dynamics method (MD). Our analysis shows that the MD simulated strengths clearly follow the $(1+n)^{-1/2}$ dependence predicted by QFM at a broad temperature range from 300 K to 4000 K. Compared with the MD results, the proposed theoretical model can give a reasonable prediction for the fracture behavior of the carbon nanotubes with a single crack, horizontal and vertical parallel double cracks.

Keywords: Carbon Nanotubes, Quantized Fracture Mechanics, Molecular Dynamics, Temperature Effect, Defect Dependence.

1. INTRODUCTION

Since carbon nanotubes (CNTs) were first discovered by Iijima in 1991,¹ they have been widely used in a broad range of applications because of their remarkable properties and much theoretical and experimental effort has been directed toward exploring their mechanical and physical properties.^{2–4} Recent experiments have shown the carbon nanotube to be a stronger material with fracture strength of 0.15 TPa at room temperature.⁵ The variation in the strength mainly depends on the critical size, diameter, temperature and strain rate. Temperature and strain rate have been shown to play an important role in determining the tensile strength and tensile strain of the CNTs.⁶ In addition, the tensile strength of CNTs can be reduced to 60% of the pristine tube value if vacancies are present.^{7,8}

With the impending demand of CNT integration into MEMS devices, it is important to further understand and accurately estimate the strength of carbon nanotubes under various conditions. Recently, a new energy-based theory, namely quantized fracture mechanics (QFM), that modifies continuum-based fracture mechanics using the finite differences instead of the differentials in the Griffith's energy balance, has been developed and believed as a strong theoretical tool to analyze the mechanical properties of nanostructured materials.⁹ Zhao and Aluru¹⁰ investigated the variation in fracture strength of graphene with

temperature, strain rate, and crack length using molecular dynamics (MD) simulation and QFM method. Pugno and Ruoff¹¹ compared the fracture strengths predicted by QFM with experimental and atomic simulated results on carbon nanotubes. More recently, Pugno¹² reviewed the research progress on prediction of fracture strengths for carbon nanotubes with a single crack via the QFM method and atomic simulations. Therefore a deeper understanding the validity of applying the QFM method to predict the fracture properties of closed-end CNTs with different defect shapes over a broad range of temperatures and strain-rates is necessary and of great importance.

The purpose of the present study is to propose a theoretical approach for understanding the dependence of fracture strength of CNTs with different defect shapes over a broad range of temperatures. A theoretical framework is developed for fracture strength and fracture strain as a function of temperature and strain rate for CNTs based on the kinetic analysis of fracture and then the quantized fracture mechanics is applied to estimate the fracture behavior of the defective CNTs. Lastly, MD simulations are also used to validate our theoretical approaches.

2. KINETIC ANALYSIS OF FRACTURE

Following the procedure detailed by Zhao and Aluru,¹⁰ we investigate the fracture properties of CNTs using the kinetic analysis of fracture (KAF). Unlike the nonlinear stress–strain relations of graphene,¹⁰ our MD simulations

*Authors to whom correspondence should be addressed.

show that there is a remarkable flat step in the nonlinear stress–strain curves of CNTs, which was also observed by Ragab and Basaran.¹³ Therefore, we define $\sigma(t)$ under constant strain rate $\dot{\epsilon}$ as a double Boltzmann function, i.e.,

$$\sigma(t) = \sigma_0 + A \left(\frac{p}{1 + \exp(\dot{\epsilon}t - h_1/k_1)} + \frac{1-p}{1 + \exp(\dot{\epsilon}t - h_2/k_2)} \right) \quad (1)$$

where σ_0 , A , p , h_1 , h_2 , k_1 and k_2 are constants obtained by fitting the MD simulated stress–strain data in the present study.

Using the trapezoidal integration, the failure time t_r can be expressed as

$$\int_0^{t_r} \frac{n_s}{\tau_0 [\exp(U - KV\sigma(t)/kT)]} dt \approx \frac{t_r}{4} \left(\frac{n_s}{\tau_0 [\exp(U - KV\sigma(t_r)/kT)]} + \frac{2n_s}{\tau_0 [\exp(U - KV\sigma(t_r/2)/kT)]} + \frac{n_s}{\tau_0 [\exp(U - KV\sigma(0)/kT)]} \right) = 1 \quad (2)$$

where τ_0/n_s is the pre-exponential factor, τ_0 is the vibration period of atoms in solid, n_s is defined as the number of sites available for the state transition, U is the interatomic bond dissociation energy, V is the activation volume, K is the coefficient of local overstress, and k is the Boltzmann constant.

The failure time t_r can be solved numerically according to Eq. (2) with the iteration technology. The fracture strain ϵ_r can be expressed as a function of t_r , i.e.,

$$\epsilon_r = \dot{\epsilon}t_r \quad (3)$$

For a nonlinear elastic (NLE) material, the fracture strength σ_r is defined as

$$\sigma_r = \sigma_0 + A \left(\frac{p}{1 + \exp(\dot{\epsilon}t_r - h_1/k_1)} + \frac{1-p}{1 + \exp(\dot{\epsilon}t_r - h_2/k_2)} \right) \quad (4)$$

Whereas for a linear elastic (LE) material, the fracture strength σ_r is directly defined as

$$\sigma_r = K\dot{\epsilon}t_r \quad (5)$$

With the application of QFM, for CNTs with an n -atom ($n \approx 1-10$) defect, the fracture strength σ_f for a nanotube having atomic size a (the fracture quantum) and containing a crack perpendicular to the applied load (nanotube axis) is given by Ref. [11]

$$\sigma_f = \sigma_r(\dot{\epsilon}, T) \sqrt{1 + \frac{\rho}{2a}(1+n)^{-1/2}}, \quad n > 0 \quad (6)$$

where ρ is tip radius, and σ_r is the theoretical defect-free nanotube strength calculated by Eq. (4). For a linear chain of n removed atoms,¹¹ $2\rho \approx a$.

For two parallel n -missing defects in a CNT (shown in Fig. 1), we define the fracture strength σ_f as

$$\sigma_f = \alpha \sigma_r(\dot{\epsilon}, T) \sqrt{1 + \frac{\rho}{2a}(1+n_p)^{-1/2}}, \quad n_p > 0 \quad (7)$$

where n_p is defined as the sum of missing atoms perpendicular to the applied load. Note that n_p equals to the sum of missing atoms of two cracks in case of horizontal parallel double cracks (Fig. 1(a)) and to the number of missing atoms of each crack in case of vertical parallel double cracks (Fig. 1(b)).

Refer to the continuum fracture mechanics, we define the factor α of adjacent-defect interaction as,

$$\alpha = \begin{cases} \sqrt{\left(\frac{L}{\pi b} \tan \frac{\pi b}{L}\right)} & \text{for horizontal parallel double cracks shown in Figure 1(a)} \\ \sqrt{\left(\frac{L}{\pi b} \tanh \frac{\pi b}{L}\right)} & \text{for vertical parallel double cracks shown in Figure 1(b)} \end{cases} \quad (8)$$

where L is the center distance between two adjacent cracks, and $2b$ is crack length perpendicular to the applied load, as shown in Figure 1. For a single crack, $L \gg b$, so $\alpha = 1$.

3. MOLECULAR DYNAMICS MODEL

In order to obtain the stress–strain curve for the kinetic analysis of fracture mentioned above, MD simulations are

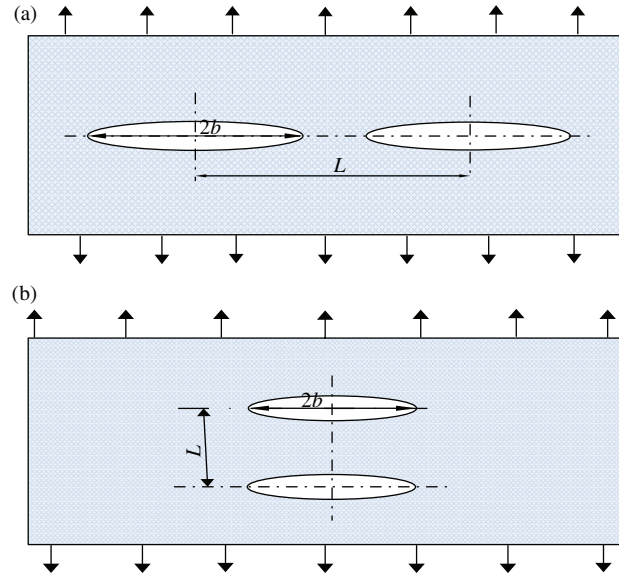


Fig. 1. Sketches of (a) horizontal and (b) vertical parallel double cracks perpendicular to the applied load

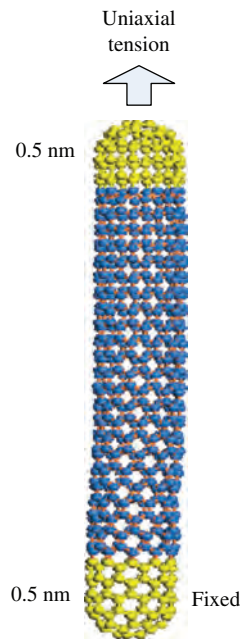


Fig. 2. A closed-end (10, 0) CNT under uniaxial test.

performed using LAMMPS,¹⁴ in which the Nose-Hoover thermostat is employed to holding temperature and the Verlet algorithm is applied to calculate the atoms' trajectories. We perform Isothermal-Isobaric (NVT) simulations at the specified temperature for 100 ps with a time step of 1 fs to let the system reach its equilibrium configuration. Then, we perform the deformation simulation controlled along the axial direction of the structure by applying a strain rate in a range of $1.4 \times 10^{-5} \text{ ps}^{-1}$ to $1.4 \times 10^{-2} \text{ ps}^{-1}$. A closed-end (10, 0) zigzag carbon nanotube with a length of 68.42 \AA is established, as shown in Figure 2. The length of C–C bond is 0.142 nm and the total number of the carbon atoms is 640.

The Tersoff potential¹⁵ is adopted to calculate the atomic interactions between the carbon atoms. The total energy of the system in the Tersoff potential can be expressed as

$$E = \frac{1}{2} \sum_i \sum_{i \neq j} V_{ij} \quad (9)$$

The pairwise potential energy V_{ij} , is defined as

$$V_{ij} = f_c(r_{ij}) [f_R(r_{ij}) + b_{ij} f_A(r_{ij})] \quad (10)$$

where $f_c(r)$ is a smooth cutoff function, $f_R(r)$ and $f_A(r)$ are the attractive and repulsive pair potential, respectively, and b_{ij} is a modified factor.

4. RESULTS AND DISCUSSION

4.1. Temperature Dependence

To compare our theoretical results calculated from the proposed double Boltzmann function with MD simulated results, we predict the theoretical fracture strengths for

fracture strain and fracture strength with the NLE constitutive relation. We use $\tau_0 = 10^{-13} \text{ s}^{10}$ as the average vibration period of atoms in solid. According to the Tersoff potential, we define $U = 4.48 \text{ eV}$, $V = 8.16 \text{ \AA}^3$, and $K = 0.6$. The stress–strain relations obtained from MD simulations, as shown in Figure 3, have a slight discrepancy with temperature. Therefore, using the least-squares technique according to the MD simulated stress–strain curve at temperature 300 K, we can get the fitted parameters (i.e., $\sigma_0 = -1600.83$, $A = 1743.97$, $p = 0.96$, $h_1 = -0.17$, $h_2 = 0.15$, $k_1 = -0.057$ and $k_2 = -0.017$) of Eq. (1) $n_s = 1.5 N$ is defined as the total number of bonds that can be broken in an N -atom system. In this study, we build an atom system with $N = 640$.

The strain rate is fixed as 0.0014 ps^{-1} to investigate the temperature dependence in MD simulations. The stress–strain relations for various temperatures ranging from 300 K to 4000 K are shown in Figure 3. The theoretical fitted stress–strain curve is also given in Figure 3. As shown in Figure 3, a NLE behavior with a significant flat step is observed for CNTs and this flat step gradually vanish when the temperature is above 2000 K.

Moreover, the transition time, fracture strain and fracture strength are calculated with Eqs. (2)–(4) in the KAF approach, while they are also comparably obtained from the MD simulations in the MD model. We note that only the MD simulated stress–strain curve at the temperature of 300 K is used for fitting the fitted parameters of Eq. (1) in the KAF approach. Figure 4 shows the variation in the fracture strength as a function of temperature for the MD results and the KAF theoretical approximations with both the LE and NLE models are presented. Clearly, with the temperature increases, the fracture strength of the CNT decreases, as shown in Figures 3 and 4. When the temperature is 300 K, for example, the fracture strength of the CNT is about 140 GPa and its elongation is about 0.21, which agrees well with the experiment result.⁵ In addition, the NLE theoretical model can obviously provide a

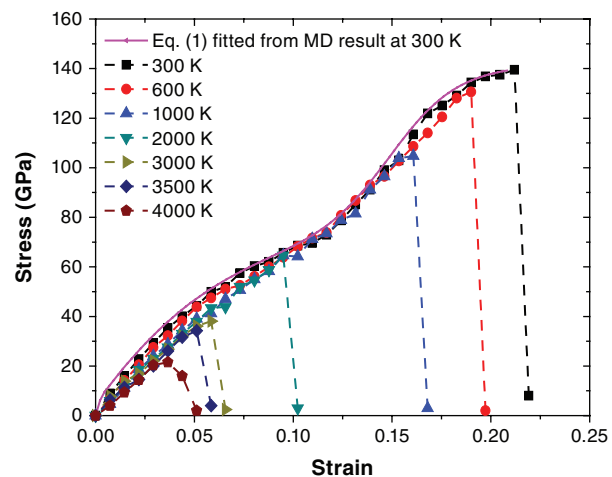


Fig. 3. The NLE stress–strain relations at varied temperatures.

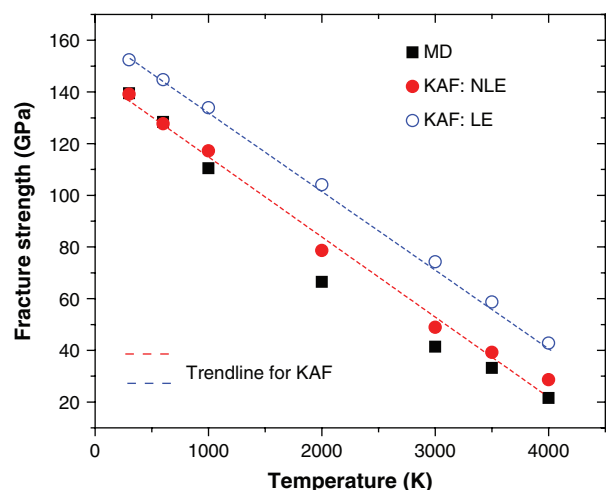


Fig. 4. Fracture strengths as a function of the temperature. The symbol MD, KAF: NLE and KAF: LE represent the MD simulated curve, NLE curve and LE curve, respectively.

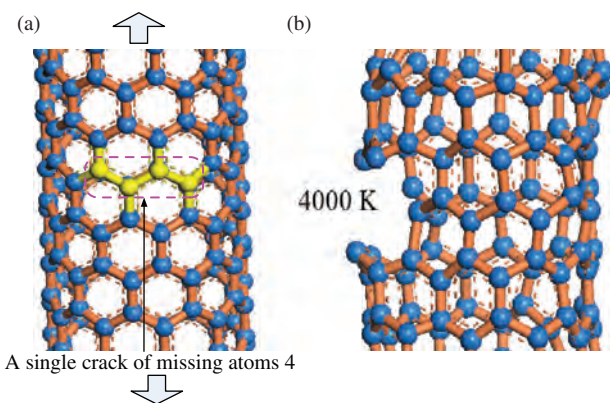


Fig. 5. (a) A defective closed-end (10, 0) CNT with a single crack of 4 missing atoms, and (b) The atomic configuration around the vacancy location in the CNT with an 4-atom defect at 4000 K.

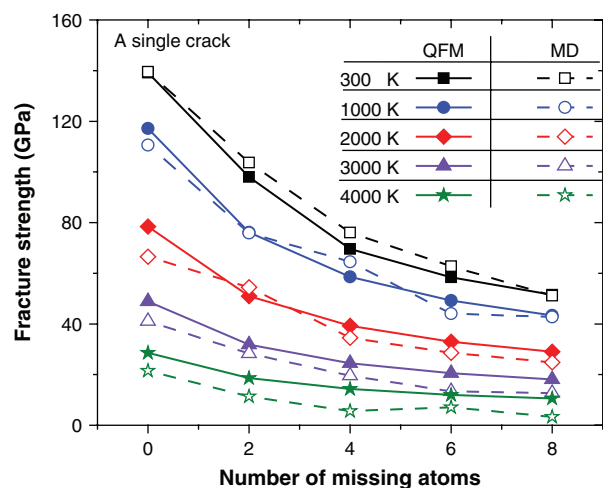


Fig. 6. Variation of fracture strength with respect to the number of missing atoms for CNTs with a single crack in a broad temperature range from 300 K to 4000 K.

better estimate of all the fracture properties than the LE theoretical model, which is validated by the MD simulated results.

4.2. Defect Dependence

Generally defects will be existed in the CNTs during fabrication. Therefore, to systematically investigate the effect of defects, especially missing atoms, on the fracture strength of the CNTs, we estimate a defective closed-end (10,0) zigzag carbon nanotube with a length of 68.42 Å, as shown in Figure 5(a). First, an n -atom defect is created by removing n adjacent atoms along the circumference of the nanotube; two-, four-, six- and eight-atom defects are then treated. After initial equilibration of these structures, a strain rate of 0.0014 ps^{-1} is applied to perform the uniaxial tensile test in a broad temperature range from 300 K to 4000 K. Figure 5(b) gives the atomic configuration around the vacancy location in the CNT with an 4-atom defect at 4000 K, from which we can find that the C atoms could still keep sp^2 bonds at a temperature as high as 4000 K.

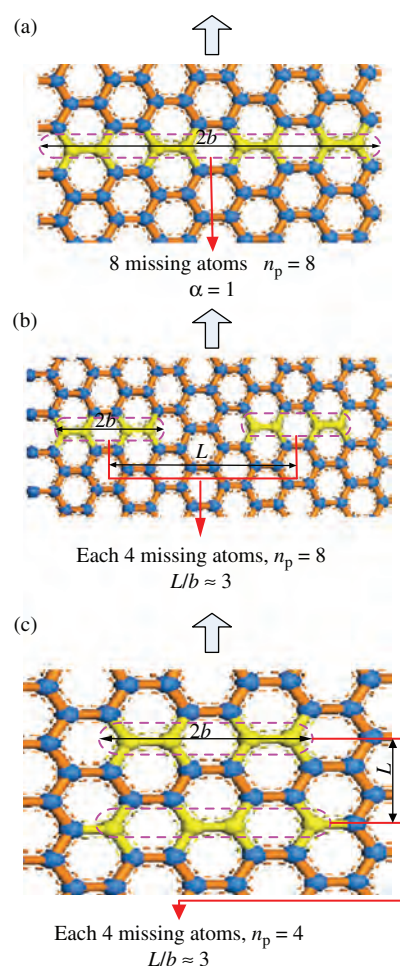


Fig. 7. Schematic diagrams of the (10, 0) CNT with missing 8 atoms, (a) a single crack with 8 missing atoms, (b) horizontal parallel double cracks with each 4 missing atoms, and (c) vertical parallel double cracks with each 4 missing atoms.

Table I. Fracture strengths of defective closed-end CNTs with different defect styles corresponding to Figures 5 and 7.

	Defect-free	Figure 7			Figure 5
	$n_p=0$	$n_p=8$	$n_p=8$	$n_p=4$	A single crack of 4-missing atoms
MD results	139.2	51.1	67.2	64.1	72.1
Equation (9)	139.6	52.0	66.9	60.3	69.8

The comparison between the MD simulations and QFM results obtained from Eq. (7) is plotted in Figure 6, which indicates that the MD simulated strengths decrease with the increasing number of missing atoms, and clearly follow the $(1+n)^{-1/2}$ dependence predicted by QFM at a broad temperature range.

Secondly, uniaxial tensile tests of CNTs with assuming defects including a single crack, horizontal and vertical parallel double cracks (especially shown in Figs. 7(a)–(c)) are also performed to investigate the influence of defect style at the temperature of 300 K and the strain rate of 0.0014 ps^{-1} . Figure 7 shows the sketches of defects and lists the values of L/b and n_p . We note that n_p equals to 8 in Figure 7(b) (i.e., the sum of missing atoms of two cracks in case of horizontal parallel double cracks), and equals to 4 in Figure 7(c) (i.e., the number of missing atoms of each crack in case of vertical parallel double cracks). Using Eq. (7), we can calculate the QFM theoretical fracture strengths for comparison. The comparison between MD data and QFM results is listed in Table I. The theoretical results show a reasonable agreement with the MD results. It can be found that the proposed theoretical model can give a reasonable prediction for the fracture behavior of carbon nanotubes with a single crack, horizontal and vertical parallel double cracks.

5. CONCLUSIONS

A theoretical model is proposed to predict the fracture strength and fracture strain as a function of temperature and strain rate for carbon nanotubes based on kinetic analysis of fracture, with the validity of molecular dynamics method. Firstly, the theoretical results show a reasonable agreement with the molecular dynamics results. Secondly, both of the theoretical and numerical results show that temperature plays an important role in determining the fracture properties of closed-end CNTs.

The influences of assuming defects including a single crack, horizontal and vertical parallel double cracks on the fracture properties of closed-end CNTs are also investigated using quantized fracture mechanics (QFM) theory

and molecular dynamics method. Uniaxial tensile tests of the carbon nanotubes with a single crack and parallel double cracks are especially examined. The MD simulated strengths decrease with the increasing number of missing atoms, and clearly follow the $(1+n)^{-1/2}$ dependence predicted by QFM at a broad temperature range. The proposed theoretical model can give a reasonable prediction for the fracture behavior of closed-end CNTs with a single crack, horizontal and vertical parallel double cracks in a broad temperature range from 300 K to 4000 K.

Acknowledgments: This work was supported by the National Natural Science Foundation of China (Grant Nos. 11162014 and 11372126), and the 973 Program of MOST of 2010CB631005.

References

1. S. Iijima, Helical microtubules of graphitic carbon. *Nature* 354, 56 (1991).
2. G. M. Neelgund and A. Oki, Deposition of silver nanoparticles on dendrimer functionalized multiwalled carbon nanotubes: Synthesis, characterization and antimicrobial activity. *J. Nanosci. Nanotechnol.* 11, 3621 (2011).
3. J. P. Lu, Elastic properties of carbon nanotubes and nanoropes. *Phys. Rev. Lett.* 79, 1297 (1997).
4. G. F. Close, S. Yasuda, B. Paul, S. Fujita, and H. S. P. Wong, A 1 GHz integrated circuit with carbon nanotube interconnects and silicon transistors. *Nano Lett.* 8, 706 (2008).
5. B. G. Demczyk, Y. M. Wang, J. Cumings, M. Hetman, W. Han, A. Zettl, and R. O. Ritchie, Fabrication and mechanical properties of multi-walled carbon nanotubes/epoxy nanocomposites. *Mater. Sci. Eng. A* 334, 173 (2002).
6. C. Wei, K. Cho, and D. Srivastava, Tensile strength of carbon nanotubes under realistic temperature and strain rate. *Phys. Rev. B* 67, 115407 (2003).
7. M. Sammalkorpi, A. Krashennnikov, A. Kuronen, K. Nordlund, and K. Kaski, Mechanical properties of carbon nanotubes with vacancies and related defects. *Phys. Rev. B* 70, 245416 (2004).
8. S. Zhang, S. L. Mielke, R. Khare, D. Troya, R. Ruoff, G. C. Schatz, and T. Belytschko, Mechanics of defects in carbon nanotubes: Atomistic and multiscale simulations. *Phys. Rev. B* 71, 115403 (2005).
9. N. Pugno and R. Ruoff, Quantized fracture mechanics. *Philos. Mag.* 84, 2829 (2007).
10. H. Zhao and N. R. Aluru, Temperature and strain-rate dependent fracture strength of graphene. *J. Appl. Phys.* 108, 064321 (2010).
11. N. Pugno, The role of defects in the design of space elevator cable: From nanotube to megatube. *Acta Mater.* 55, 5269 (2007).
12. N. Pugno, A review on the design of superstrong carbon nanotube or graphene fibers and composites, *Nanotube Superfiber Materials: Changing Engineering Design* (2014), pp. 495–518.
13. T. Ragab and C. Basaran, Joule heating in single-walled carbon nanotubes. *Appl. Phys.* 106, 063705 (2009).
14. S. Plimpton, Fast parallel algorithms for short-range molecular dynamics. *Comput. Phys.* 117, 1 (1995).
15. J. Tersoff, Modeling solid-state chemistry: Interatomic potentials for multicomponent systems. *Phys. Rev. B* 39, 5566 (1989).

Received: 9 October 2014. Accepted: 15 October 2014.